NACA RM L52B12

NACA

RESEARCH MEMORANDUM

TRANSONIC DRAG CHARACTERISTICS AND PRESSURE DISTRIBUTION ON THE BODY OF A WING-BODY COMBINATION CONSISTING OF A BODY OF REVOLUTION OF FINENESS RATIO 12 AND A WING HAVING SWEEPBACK OF 45°, ASPECT RATIO 4, TAPER RATIO 0.6, AND NACA 65A006 AIRFOIL SECTIONS

By Max C. Kurbjun and Jim Rogers Thompson

Langley Aeronautical Laboratory
Langley Field, Va.

NATIONAL ADVISORY COMMITTEE FOR AERONAUTICS

WASHINGTON
April 8, 1952

NATIONAL ADVISORY COMMITTEE FOR AERONAUTICS

RESEARCH MEMORANDUM

TRANSONIC DRAG CHARACTERISTICS AND PRESSURE DISTRIBUTION ON THE BODY OF A WING-BODY COMBINATION CONSISTING OF A BODY OF REVOLUTION OF FINENESS RATIO 12 AND A WING HAVING SWEEPBACK OF 45°, ASPECT RATIO 4, TAPER RATIO 0.6, AND NACA 65A006 AIRFOIL SECTIONS

By Max C. Kurbjun and Jim Rogers Thompson

SUMMARY

In order to evaluate recently developed testing techniques for near sonic speeds, the National Advisory Committee for Aeronautics is conducting a series of directly comparable tests by different test methods. As part of this program, the drag and pressure distribution have been measured near zero lift for a wing-body combination consisting of a body of fineness ratio 12 and a wing of 45° sweepback having an aspect ratio of 4, a taper ratio of 0.6, and NACA 65A006 airfoil sections in the direction of flight. The measurements were made by the free-fall method and extend from a Mach number of 0.75 to a Mach number of 1.16.

The results obtained revealed that the principal effect of the presence of the wing was the superposition on the body pressure distribution of an additional pressure distribution having the same shape as that expected at the root of a swept wing. For the investigated configuration, this superposition reduced the critical Mach number of the body. The body drag rise and the flow changes associated with transition through the speed of sound occurred in the same manner as on a similar body without wings (NACA RM L9J27) except at a slightly lower Mach number because of the lower critical Mach number of the wing-body combination. The presence of the wing resulted in an unfavorable interference effect on the body drag which was a maximum during the abrupt drag rise.

The free-fall results were in generally satisfactory agreement with results obtained for similar configurations from tests of a rocket-powered model and from tests in the 8-foot high-speed wind tunnel.

INTRODUCTION

Recent developments in testing techniques for near sonic speeds have increased the need for directly comparable test results obtained by different methods which can be used to evaluate new testing facilities. With this objective, similar wing-body combinations are being tested by several facilities of the Langley Laboratory. The wing-body combination selected consisted of a body of revolution of fineness ratio 12 which has been used in previous free-fall tests (for example, references 1 and 2) and a wing having sweepback of 45°, an aspect ratio of 4, a taper ratio of 0.6, and NACA 65A006 airfoil sections in the direction of flight. This configuration is considered representative of the current trend in the transonic airplane design.

Results of drag measurements made by the rocket-powered-model technique for the subject configuration at Mach numbers between 0.9 and 1.5 are reported in reference 3. Results of force and pressure-distribution measurements of the configuration in the Langley 8-foot high-speed tunnel at Mach numbers between 0.6 and 0.96 and at 1.2 are reported in references 4 and 5, respectively. The subject paper presents results of free-fall tests of the configuration at Mach numbers between 0.75 and 1.16. The corresponding range of Reynolds number (based on the wing mean aerodynamic chord) was 3×10^6 to 12×10^6. The measurements were made at approximately zero lift and included total and component drags and limited body pressure-distribution data.

The free-fall results presented herein are compared with the results obtained in other facilities (references 3 to 5) and results of previous free-fall tests.

METHOD

The test was performed by utilizing the free-fall method (described in references 1 and 2) in which the flight path of the freely falling body is obtained by radar and phototheodolite equipment and other required quantities are measured at the body by means of the NACA radio-telemeter system.

Model.- The model consisted of a body-tail combination identical with those used in previous free-fall tests and sweptback wing located so that the 25-percent-chord point of the mean aerodynamic chord was located at the body maximum diameter. The wing had a sweepback of 45° (measured at the 25-percent chord line), an aspect ratio of 4, a taper ratio of 0.6, and NACA 65A006 airfoil sections in planes parallel to the direction of flight. Details and dimensions of the model are given in figure 1 and the coordinates of the body surface and orifice locations are given in tables I and II, respectively. A photograph of the model is presented as figure 2.

Measurements.- In addition to the measurement of the flight path of the test body, which was obtained from the radar and phototheodolite equipment, the following quantities were telemetered from the body: longitudinal acceleration, wing drag, tail drag, total and static pressure at airspeed head, and pressure at 18 flush orifices located on the body surface. Except for the measurement of the body pressure distribution, the instruments used were similar with those described in references 1 and 2. The body pressures were measured through a mechanical switching device which alternately connected each of nine orifice tubes to a single pressure cell. Two separate switch-cell units were provided so that a total of 18 pressures were measured at a rate of about two complete cycles per second. This system has the advantage that only two differential cells are connected to the airspeed boom static orifices and thus the lag is minimized. In addition, once each cycle the two sides of each cell were vented together in order to provide a positive check for drift in the telemeter system.

Precision of measurements.- Values of the estimated maximum uncertainty of the drag parameters obtained from the basic telemetered measurements are presented in the following table for several Mach numbers. The uncertainties given refer to coefficients based on the total wing plan area.

Drag parameter	Mach number			
	0.75	0.95	1.05	1.15
$C_{D_{total}}$	±0.0009	±0.0007	±0.0006	±0.0006
$C_{D_{wing}}$	±.0013	±.0007	±.0005	±.0003
$C_{D_{tail}}$	±.0006	±.0003	±.0002	±.0002
$C_{D_{body}}$	±.0022	±.0010	±.0008	±.0007

The estimated maximum uncertainty in the values of Mach number is less than ±0.01 and that of the body pressure coefficients decreases from about ±0.013 at a Mach number of 0.95 to ±0.005 at 1.15.

The accuracy of the total drag obtained from the retardation measurements is confirmed by the excellent agreement of the variation with time of the velocity and altitude obtained by integration of the vector sums of the measured and gravitational accelerations with the corresponding variations obtained from the radar and phototheodolite equipment. The variation of Mach number with time used herein was computed from the velocity data just described by use of atmospheric wind and temperature data. The accuracy of this Mach number is confirmed as in reference 1 by the passage over the static orifices located on the nose boom of the body bow wave at a Mach number of about 1.005.

RESULTS

The basic measurements made during the free-fall test of the model are presented in figures 3 to 5. They have been reduced to coefficient form through the use of the variation of atmospheric pressure and temperature with altitude obtained during the descent of the airplane from altitude immediately following the test.

Drag measurements.- The variation with Mach number of the total drag of the configuration as measured by the longitudinal accelerometer is presented on figure 3. The total drag coefficient was constant at a value of about 0.010 from a Mach number of 0.75 until a Mach number of 0.91 was reached. As the Mach number increased above 0.91, the total drag coefficient increased at an increasing rate and attained a value of 0.028 at a Mach number of unity. Above unity, the total drag coefficient increased gradually to 0.030 at a Mach number of 1.15. The measured division of the total drag among the component parts of the configuration is also shown on figure 3. At supersonic speeds the wing contributes about 40 percent, the body 45 percent, and the tail surfaces 15 percent of the total drag.

The variation with Mach number of the measured wing drag is shown separately in coefficient form on figure 4. The wing drag coefficient is approximately constant at 0.004 until a Mach number of about 0.95 is attained. As the Mach number increased from 0.95 to 1.00, the wing drag coefficient increased smoothly from 0.004 to 0.0105. At supersonic speeds the wing drag increased slowly and reached a value of 0.0135 at a Mach number of 1.15.

The cause of the irregularities evident in the supersonic part of the wing drag curve has not been determined; however, it should be noted that the irregularities are of the order of the estimated maximum uncertainty of the measurement.

Pressure measurements.- The variation with Mach number of the pressure measured at each orifice is presented in figure 5. The pressure coefficients plotted are, of course, the difference between the pressure at a body orifice and the pressure at the nose-boom static orifice expressed as a fraction of dynamic pressure. As in reference 1, the nose-boom static pressure is assumed correct. The validity of this assumption is discussed in reference 1.

As noted in the section entitled "Precision of Measurements," the maximum uncertainty of the pressure measurements decreases as the Mach number is increased. Data, therefore, are not presented for Mach numbers below 0.7 when the uncertainties are large compared to the measured quantity. The oscillations evident near the beginnings of most of the curves of figure 5 are of the same order or less than the quoted maximum uncertainty and are therefore not significant.

Lines showing the pressure coefficient corresponding to the local speed of sound are also shown on figure 5. Comparison of these lines with the experimental data indicates that the critical Mach number of the body in the presence of the wing is about 0.91 (fig. 5(e), $\frac{x}{l} = 0.5125$, 255°).

DISCUSSION

Pressure Data

In order to illustrate the over-all characteristics of the flow about the body of the wing-body combination, the basic data presented on figure 5 are cross-plotted in figure 6 as the variation of local Mach number along the body surface for values of free-stream Mach number between 0.84 and 1.16 in increments of 0.02. At stations where orifices were located at two or three radial positions around the body, the average pressure coefficient was used to determine the local Mach number. Because of the relatively wide spacing of these orifices and the arbitrary averaging procedure, the smooth fairings fitted to the data of figure 6 may not show the exact location and slope of rapid changes along the body. The fairings show, however, the salient features of the flow.

The shapes of the curves of figure 6 are similar to those presented in reference 1 for the body without wings except near the wing root where the curves are modified in the manner which would be expected by superposition of an additional pressure distribution having the same shape as that normally measured at the root of a swept wing. The slope of the variation of local Mach number across the region of the wing root

increases rapidly as the Mach number approaches unity. Below a Mach number of 0.96 the local Mach number decreases rapidly near the wing trailing edge; however, between Mach numbers of 0.96 and 1.00, the principal part of this rapid decrease in local Mach number moves rearward a distance of more than 1 root chord length. The transition from a subsonic to a supersonic type of pressure distribution, which was shown for a body without wings (reference 1) to be characterized by the occurrence and rapid rearward motion of a shock wave at the rear of the supersonic region and to be concomitant with the drag rise, occurs in the same manner for the wing-body combination. Reference 1 showed that for the body alone the transition phenomena occurred between Mach numbers of 0.98 and 1.00.

For detailed study of the flow over the body the basic data of figure 5 are cross-plotted on figure 7 in the form of pressure coefficient P against orifice location x/l for several Mach numbers. A fairing is fitted to the data for orifices located in the plane 90° from the plane of the wing. Data from orifices located in other planes are included as test points to show the radial variation of pressure around the body. The pressure-distribution data are compared with results for the body tested without wings (reference 1) and with theoretical results (references 1 and 6). The distributions for each speed range are discussed separately.

Subcritical speeds.- Pressure distributions for the body of the wing-body combination at Mach numbers of 0.75 and 0.90 are presented as parts (a) and (b) of figure 7. The critical Mach number of the body (see section entitled "Results") is about 0.91. Examination of these figures reveals that, except in the immediate vicinity of the wing root and at the extreme rear, the pressure distributions of the body of the wing-body combination are in good agreement with the pressure distributions for the body without wings. In the region of the wing root, the result is similar to that which would be obtained by superposition of an additional pressure distribution having the same shape as that normally obtained (for example, see reference 7) at the root of a swept wing on that of the body. The effect on the body pressure distribution due to the presence of the wing decreases rapidly both forward and rearward of the wing-fuselage juncture. As the pressures behind and in the same plane as the wing do not differ appreciably from those at the same body station but located in other planes, it is apparent that there is no separated wake on the body from the wing root. The pressure recovery at the extreme rear of the body is relatively large and indicates that no appreciable amount of flow separation occurred on the body. The pressure recovery was not, however, as large as that measured for the body alone. As the subject measurements agree closely with the theoretical results, and as other unpublished free-fall results and recent transonic wind-tunnel results (reference 8) also agree more closely with

the theoretical results, it appears that the magnitude of the pressure recovery shown in reference 1 for this region is subject to question.

Transonic speeds.- After the critical Mach number of 0.91 is exceeded there is no significant change in the flow pattern until a Mach number of about 0.96 is exceeded. This result is evident from figures 5 and 6 and by comparison of figures 7(c) and 7(d) with 7(a) and 7(b). Between 0.96 and 0.975 (figs. 7(d) and 7(e)) however, the local region of supersonic flow over the body near the rear part of the wing has expanded and the gradients steepened to such an extent that a shock wave forms near the wing trailing edge. As may be seen from figure 5 (parts (f) to (h)) this shock wave moves rearward along the body as the Mach number is increased and, at a Mach number of about 0.99, reaches the region of the body where a relatively rapid pressure recovery exists at subcritical speeds. After the shock reaches this region $\left(\frac{x}{l} = 0.75 \text{ to } 0.80\right)$ it appears to move away from the body as no further evidence of shock appears on the body. (See fig. 5.) Confirming evidence that the shock stands away from the body in this region of flow has been obtained from schlieren photographs of similar models taken in transonic wind tunnels.

Comparison of the pressure distributions for the body of the wing-body combination with those for the body without wings (figs. 7(c) to 7(g), Mach numbers of 0.925, 0.96, 0.975, 0.99, and 1.00) shows that the mechanism of the flow change is similar in the two cases and differed only in that for the wing-body combination the transition from the subcritical flow pattern to the supersonic type begins at a lower Mach number and requires a larger change in Mach number to complete the pattern than in the case of the body without wings. This difference, of course, directly results from the lower critical Mach number of the wing-body combination (compared to that of the body alone) because of the high velocity region over the rear part of the wing.

During the rearward movement of the shock (and the rearward extension of the supersonic region) the pressure distribution over the forward part of the body does not change significantly. Immediately behind the wing there is some increase in the radial variation of pressure compared to that at subcritical speeds and is probably due to the sweeping back of the wing pressure field in the local supersonic region. Farther back, however, there is still no evidence of a separated wing wake.

As the Mach number is increased above unity there is little change in the character of the flow on the rear part of the body and the changes on the front of the body are confined to a small and gradual shift in the positive direction.

Supersonic speeds.- After the shock has reached its rearward position (near $M = 1.01$) the character of the flow remains unchanged up to the maximum Mach number reached of 1.16. At Mach numbers above 1.05 (parts (i), (j), and (k) of fig. 7) the pressure distributions agree closely with those presented in reference 1 for the body without wings except, of course, in the immediate vicinity of the wing root. The distributions are similar in shape to the theoretical distributions (references 1 and 6) except that they are shifted slightly in the positive direction. In the data of reference 1 a similar shift was observed but the existence of the shift could not be proved because of the possibility of an error in the reference level. The pressure system of the subject model differed from that of reference 1 in a manner which should reduce the possibility of a level error although of necessity the same reference pressure was used (see section entitled "Measurements"). The presence of the wing on the subject model, however, precludes strict confirmation of the level of either the measurements of reference 1 or the theoretical level. It should also be noted that recent wind-tunnel measurements for similar bodies at low supersonic and transonic speeds (references 5 and 8) have agreed more closely with the theoretical level than with the experimental level indicated by reference 1. Unfortunately, the apparent confirmation of the theoretical level by the wind-tunnel measurements is somewhat uncertain at low supersonic speeds because of the possible presence of wind-tunnel-interference effects.

The general features of the flow and the apparent mechanism of the transition from subcritical to supersonic speeds as measured both in free-fall and in wind tunnels are in good qualitative agreement with that presented in reference 1 and are consistent with theory for the appropriate speed range.

Drag Data

The measurements presented herein are sufficient to show the variation with Mach number of the drag of each component of the investigated configuration in the presence of the other components. Comparison of these component drags with results for similar components obtained in other free-fall tests and from tests in other facilities are discussed in the following paragraphs.

Body.- The variation with Mach number of the drag coefficient of the body-tail combination of the subject model (computed by subtracting the measured wing drag from the measured total drag) is presented in figure 8(a). The contribution of the stabilizing tail surfaces to the drag of the body-tail combination is shown on the lower part of the figure. Also presented in figure 8(a) are similar curves taken from

reference 1 for an externally identical body-tail combination tested without wings. Comparison of the two sets of results shows that, although the tail drag is unaffected by the presence of the wing, the body drag is considerably increased at transonic speeds by the presence of the wing. These data, reduced to the variation with Mach number of the drag coefficient of the body by subtracting out the contribution of the tail surfaces, are presented in figure 8(b). The drag of the body of the subject model first begins to differ appreciably from that of the body without wings at a Mach number of about 0.96. Reference to figure 4 shows that this Mach number is also the Mach number at which the wing drag rise began and, as discussed under section entitled "pressure data," the Mach number at which a shock first appeared at the rear of the supersonic region near the wing trailing edge. It appears, therefore, that the occurrence of an appreciably supersonic region on the wing, which presumably terminates in a shock and results in the drag rise of the wing, induces through carry-over a similar flow pattern on the body and results in the body drag rise.

The drag rise of the body of the subject model, which first became appreciable at a Mach number of about 0.96, is essentially completed at the speed of sound. The drag rise of the body without wings, however, has just begun at the speed of sound and is not completed until a Mach number of over 1.01 is reached. Although the Mach number difference between the two curves, (which varies from 0.04 to 0.03 during the transition region) is only slightly greater than the sum of the quoted uncertainties of the measurements, the passage of the body bow wave over the static orifices on the boom (previously discussed) indicates that the uncertainties in Mach number in this region are considerably smaller than the quoted values.

Because of its earlier drag rise, the drag of the body of the subject model momentarily reaches a value of twice that of the body without wings. After the abrupt drag rise is completed the drag of the body of the subject model is nearly constant and tends to decrease slightly with increase in Mach number as the maximum Mach number attained is approached. The drag of the body without wings continues to increase at a decreasing rate as the Mach number is increased beyond that at which the abrupt drag rise is completed. The presence of the wing, therefore, results in an unfavorable interference drag on the body of the subject model which increases from zero at subcritical speeds to a large value during the abrupt drag rise and then decreases rapidly with increase in Mach number to 28 percent at 1.05 and 14 percent of the drag of the body without wings at a Mach number of 1.15. As the drag of the body without wings continues to increase slowly above 1.15, it appears likely that this interference drag will continue to decrease with increase in Mach number beyond that obtained in the test of the subject model.

Wing.- No other measurements of the drag of a wing similar to that of the subject model are available either in the presence of the body or under interference-free conditions. In the tests of references 3 and 4, however, as both the drag of the complete configurations and of the complete configuration less wing were measured, the wing-plus-interference drag (including both the effect of the body on the wing and the wing on the body) can be obtained as the difference between the two measurements. The variations with Mach number of the wing-plus-interference drag obtained from references 3 and 4 for the subject configuration are presented in figure 9 where they are compared with the variation obtained from the free-fall data (subject model and reference 1). The variation with Mach number of wing drag measured in the subject test (wing-plus-body-on-wing-interference drag) is also presented. This latter variation, of course, includes the interference effect on the wing due to the presence of the body but does not (as do the other curves) also include the interference effect on the body due to the presence of the wing.

Examination of figure 9 reveals that the variation with Mach number of the wing-plus-interference drag (including both the effect of the body on the wing and the wing on the body) measured in the Langley 8-foot high-speed tunnel is in general agreement with that obtained from the subject tests and that the agreement for the rocket-powered model is somewhat less satisfactory. Just below the drag rise, the free-fall data are slightly lower than that of the other two methods. The discrepancy in this range is within the estimated uncertainty of the measurements. The Mach number at which the drag rise begins is about the same for all three sets of data; however, the drag rise measured for the rocket-powered model is somewhat more abrupt than the others. The wing-plus-interference drag for the rocket-powered model peaked at a Mach number of 0.98 whereas that for the free-fall model peaked at 1.0. The discrepancies during the abrupt drag rise are of the same order as the sum of the quoted Mach number uncertainties (± 0.01 for each test) although additional evidence (see section entitled "Results") is available which indicates that the uncertainty in the free-fall measurements near Mach number 1 is appreciably less than ± 0.01.

At supersonic speeds, the total wing-plus-interference drag obtained from the free-fall measurements first decreases and then increases slightly and a short extrapolation of the data would pass very close to the point obtained in the Langley 8-foot high-speed tunnel at a Mach number of 1.2. Data for the rocket-powered model, however, decrease above 0.98 and at a Mach number of 1.2 are 26 percent lower than those obtained from the free-fall and Langley 8-foot high-speed tunnel tests. Recent results of tests of rocket-powered models have indicated that the results for the body-alone configuration presented in reference 3 may have been affected by blistering of the lacquer finish due to the heat generated at the maximum Mach number reached (about 1.9). Unpublished

results for a rocket-powered model of the subject wing-body combination with an improved finish agreed closely with the free-fall and wind-tunnel results at the maximum Mach number attained but gave somewhat higher drags near the speed of sound.

The wing drag measured on the free-fall model (wing-plus-body-on-wing-interference drag) presented on figure 9 is always less than the wing plus total wing-body interference measured in the free-fall tests or in the Langley 8-foot high-speed tunnel. The interference effect of the presence of the wing on the body drag therefore is always unfavorable and increases from zero at subcritical speeds to a maximum near the speed of sound but decreases as the Mach number is increased above 1.0.

Wing-body configuration.- The variations with Mach number of the drag of the subject configuration as measured by the three different test facilities are compared in figure 10. The test configurations differed at the rearward end of the body because of the requirements of the test techniques. The data have been corrected for these dissimilarities in the following manner:

Free-fall model (subject model) - Measured total drag less measured tail drag.

Rocket-powered model (reference 3) - Measured total drag less estimated fin drag (reference 3) less measured base drag plus thrust on cut-off part of fuselage (computed from pressure distributions presented in references 1 and 7)

8-foot high-speed tunnel model (reference 4) - Measured total drag less base pressure drag plus thrust on cut off part of fuselage (as above).

Comparison of the variations with Mach number presented in figure 10 show the results of the three facilities to be in generally satisfactory agreement. The drag rises of the rocket-powered model and the model used in the Langley 8-foot high-speed tunnel are somewhat more abrupt and appear to start earlier than that of the free-fall model; however, the differences could be resolved by a total discrepancy of the order of 0.01 Mach number which is less than the limits of uncertainty of these measurements.

At the highest Mach number reached in the wind-tunnel and free-fall tests the total drag of the rocket-powered model is about 10 percent

lower than that obtained by the other two facilities. The discrepancy is somewhat larger than the sum of the quoted maximum uncertainties of the measurements.

CONCLUSIONS

Measurements have been made by the free-fall method of the drag and pressure distribution on a representative wing-body combination as part of a program to obtain directly comparable results which can be used to evaluate new transonic testing facilities and techniques. Results were obtained at approximately zero lift throughout the Mach number range of 0.75 to 1.16. Analysis of the results obtained led to the following conclusions:

1. The principal effect of the presence of the wing is the effective superposition on the body pressure distribution of an additional pressure distribution having the same shape as that normally obtained at the root of a swept wing. For the investigated configuration this superposition reduces the critical Mach number of the body, and when the wing drag rise begins the carry-over on to the body results in the body drag rise which occurs according to the same mechanism described for the body alone in NACA RM L9J27 but at a lower free-stream Mach number.

2. The presence of the wing results in an unfavorable interference drag on the body which increases from zero at subcritical speeds to a large value during the abrupt drag rise and then decreases rapidly to 28 percent of the drag of the body without wings at a Mach number of 1.05 and reaches a value of 14 percent at a Mach number of 1.16.

3. Comparison of the free-fall results with those obtained in the Langley 8-foot high-speed tunnel (NACA RM L50H08) and for a rocket-powered free-flight model (NACA RM L9H30) showed generally satisfactory agreement when the estimated maximum uncertainties of the various measurements are considered.

Langley Aeronautical Laboratory
National Advisory Committee for Aeronautics
Langley Field, Va.

REFERENCES

1. Thompson, Jim Rogers: Measurements of Drag and Pressure Distribution on a Body of Revolution throughout Transition from Subsonic to Supersonic Speeds. NACA RM L9J27, 1950.

2. Thompson, Jim Rogers, and Mathews, Charles W.: Effect of Wing Sweep, Taper, and Thickness Ratio on the Transonic Drag Characteristics of Wing-Body Combinations. NACA RM L8K01, 1948.

3. Katz, Ellis: Flight Investigation from High Subsonic to Supersonic Speeds to Determine the Zero-Lift Drag of a Transonic Research Vehicle Having Wings of 45° Sweepback, Aspect Ratio 4, Taper Ratio 0.6, and NACA 65A006 Airfoil Sections. NACA RM L9H30, 1949.

4. Osborne, Robert S.: A Transonic-Wing Investigation in the Langley 8-Foot High-Speed Tunnel at High Subsonic Mach Numbers and at a Mach Number of 1.2. Wing-Fuselage Configuration Having a Wing of 45° Sweepback, Aspect Ratio 4, Taper Ratio 0.6, and NACA 65A006 Airfoil Section. NACA RM L50H08, 1950.

5. Loving, Donald L., and Estabrooks, Bruce B.: Transonic-Wing Investigation in the Langley 8-Foot High-Speed Tunnel at High Subsonic Mach Numbers and at a Mach Number of 1.2. Analysis of Pressure Distribution of Wing-Fuselage Configuration Having a Wing of 45° Sweepback, Aspect Ratio of 4, Taper Ratio of 0.6, and NACA 65A006 Airfoil Section. NACA RM L51F07, 1951.

6. Thompson, Jim Rogers: A Rapid Graphical Method for Computing the Pressure Distribution at Supersonic Speeds on a Slender Arbitrary Body of Revolution. NACA TN 1768, 1949.

7. Danforth, Edward C. B., and O'Bryan, Thomas C.: Pressure-Distribution Measurements over a 45° Sweptback Wing at Transonic Speeds by the NACA Wing-Flow Method. NACA RM L51D24, 1951.

8. Hallisey, Joseph M., Jr.: Pressure Measurements on a Body of Revolution in the Langley 16-Foot Transonic Tunnel and a Comparison with Free-Fall Data. NACA RM L51L07a, 1952.

TABLE I

COORDINATES OF THE FINENESS-RATIO-12 BODY

[Nose radius, 0.060 in.]

X (in.)	Y (in.)	X (in.)	Y (in.)
0.00	0.000	48.00	4.876
.60	.277	54.00	4.971
.90	.358	60.00	5.000
1.50	.514	66.00	4.955
3.00	.866	72.00	4.828
6.00	1.446	78.00	4.610
9.00	1.936	84.00	4.274
12.00	2.365	90.00	3.754
18.00	3.112	96.00	3.031
24.00	3.708	102.00	2.222
30.00	4.158	108.00	1.350
36.00	4.489	114.00	.526
42.00	4.719	120.00	0.000

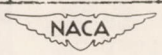

TABLE II

LOCATION OF ORIFICES ON BODY

Fraction of body length from nose, x/l	Distance from nose (in.)	Radial displacement (wing located in 90°-270° plane) (deg)
0.1625	19.50	0, 180
.3125	37.50	180
.3625	43.50	180, 255
.4625	55.50	180
.5125	61.50	180, 225, 255
.6125	73.50	180, 270
.7125	85.50	180, 225, 270
.7625	91.50	180
.8125	97.50	180, 270
.9021	108.25	180
Orifice diameter is 3/32 inch.		

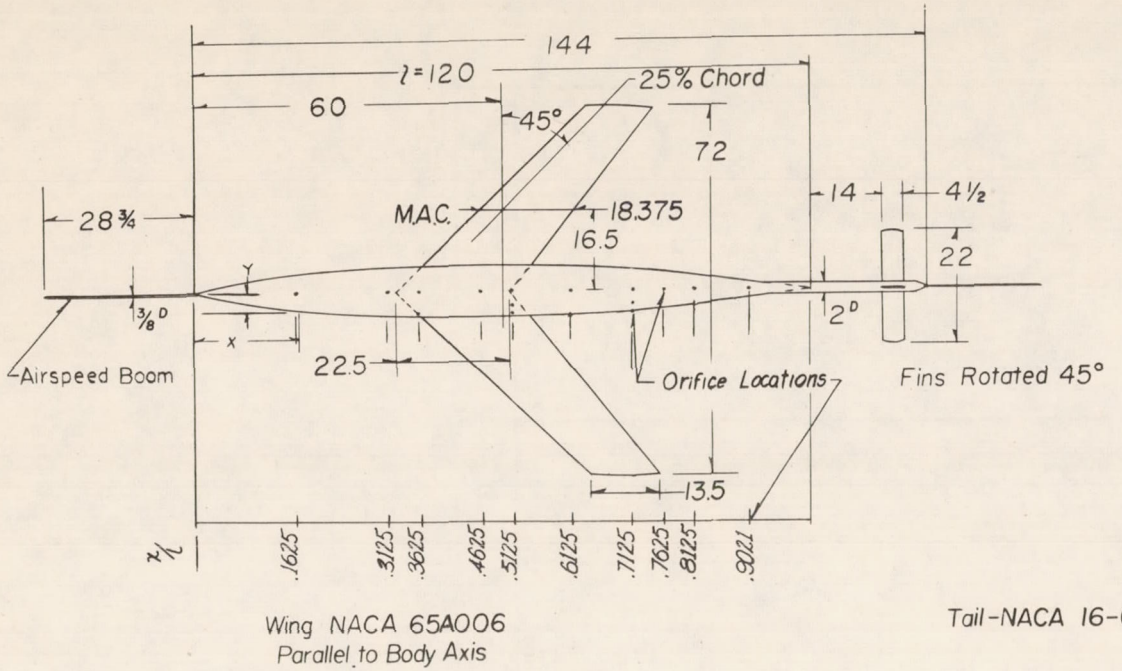

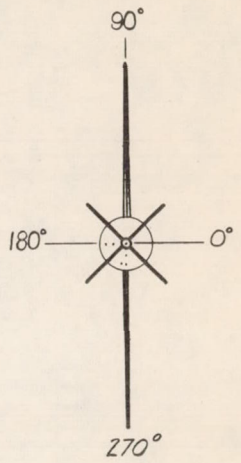

MODEL AREAS, sq. ft.

Frontal		Plan	
Body	0.545	Tail	1.232
Tail	0.074	Wing, Exposed	7.48
Wing	0.449	Wing, Total	9.00
Total Frontal	1.068	Body Surface	17.99

Figure 1.- Details and dimensions of the completed model. The coordinates of the body surface and the orifice locations are given in tables I and II, respectively. Dimensions are in inches or as noted.

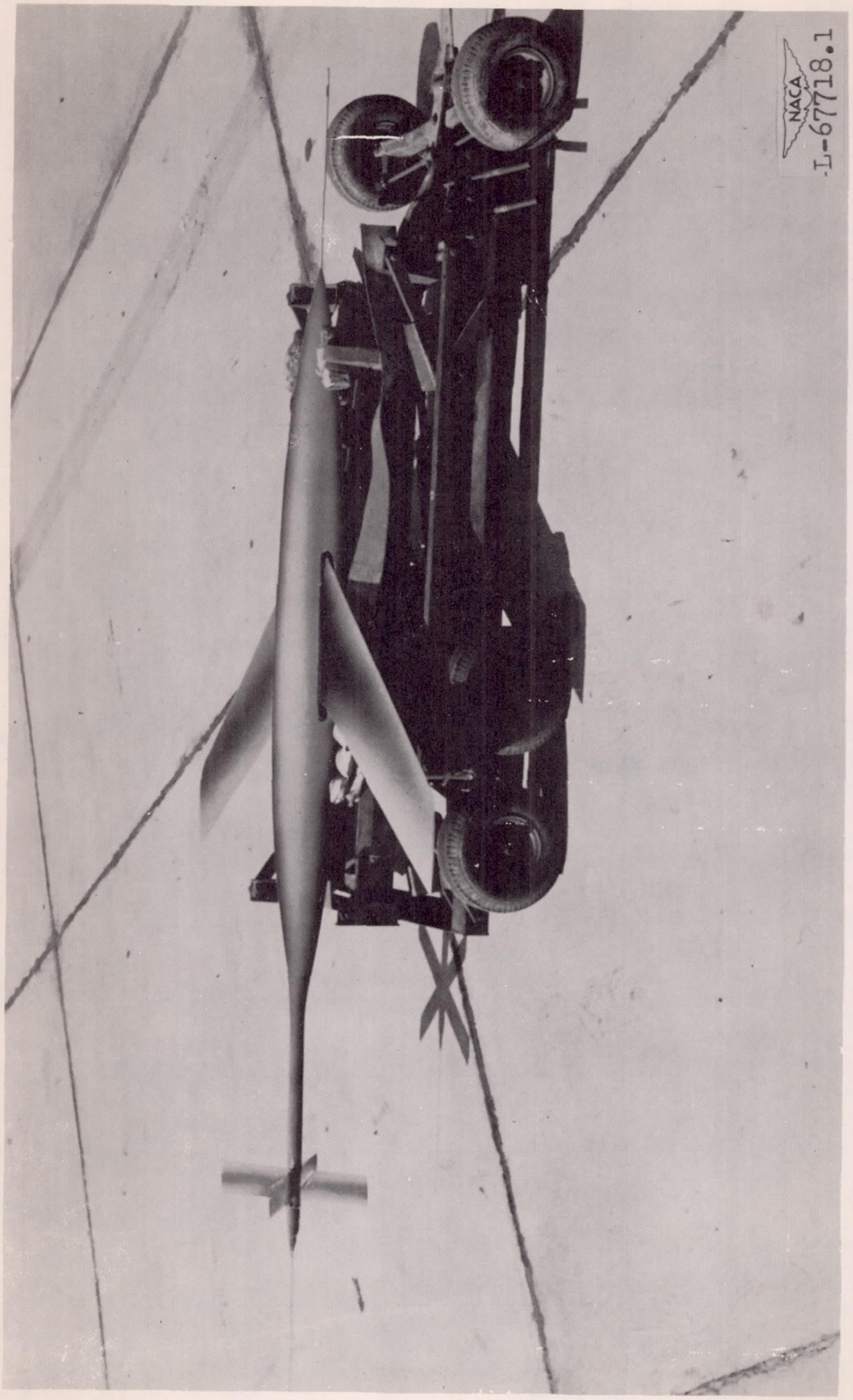

Figure 2.- Photograph of the complete free-fall model.

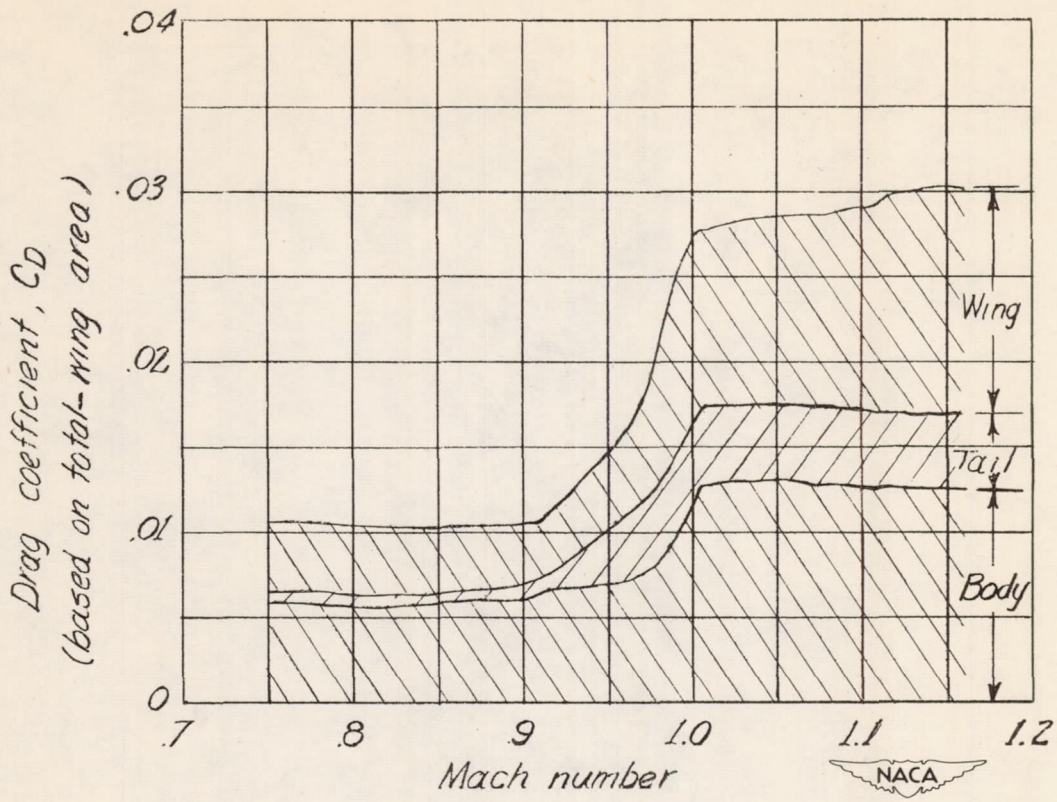

Figure 3.- Variation with Mach number of the drag coefficient of the complete wing-body combination showing the contribution of the component parts.

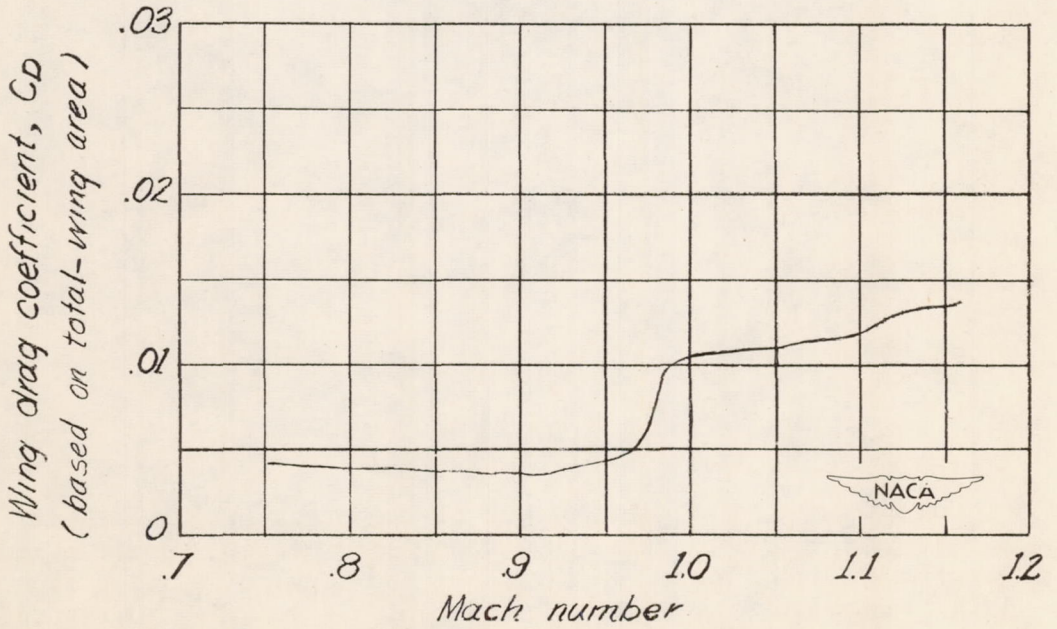

Figure 4.- Variation with Mach number of the wing-drag coefficient measured in the presence of the body.

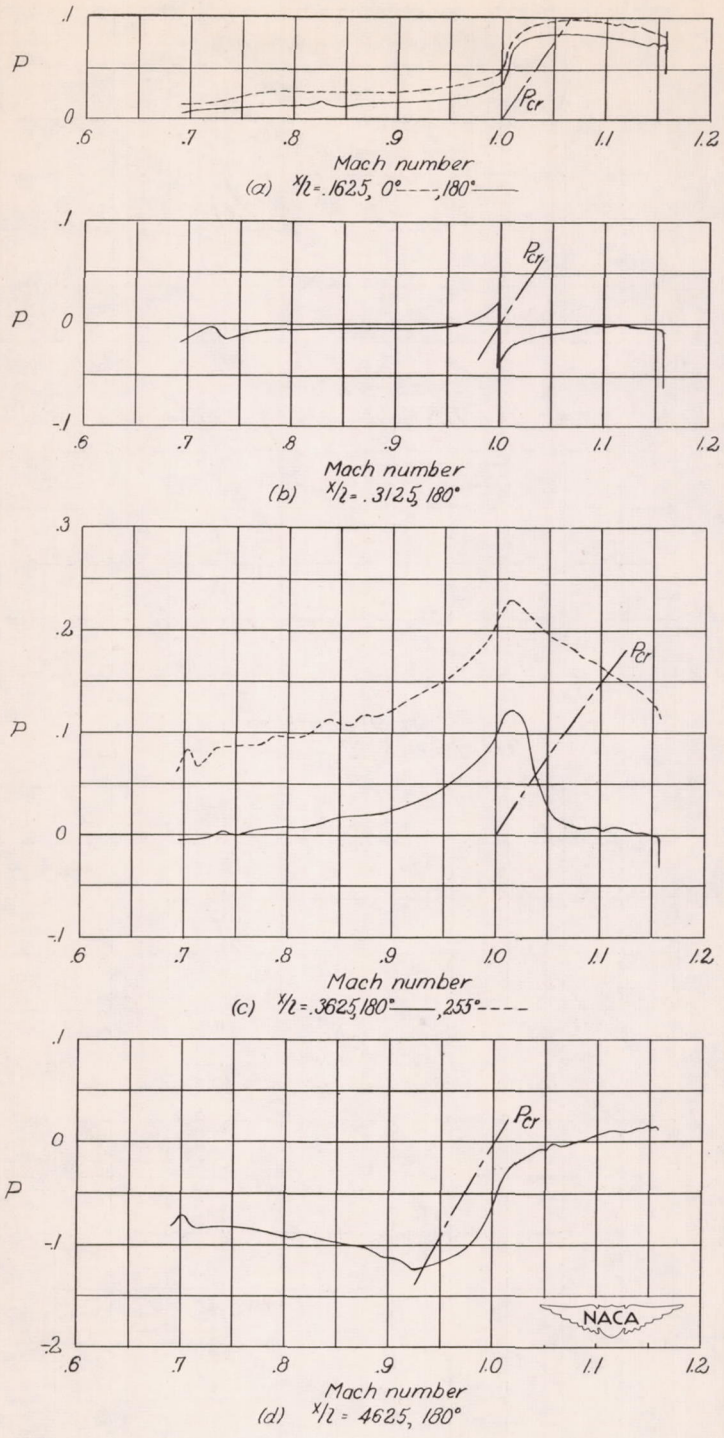

Figure 5.- The variation with Mach number of the pressure coefficient P measured at each orifice. The location of each orifice is expressed as a fraction of body length x/l and by its angular position from the plane of symmetry. (See fig. 1 and table II.) Lines corresponding to the local speed of sound are also shown.

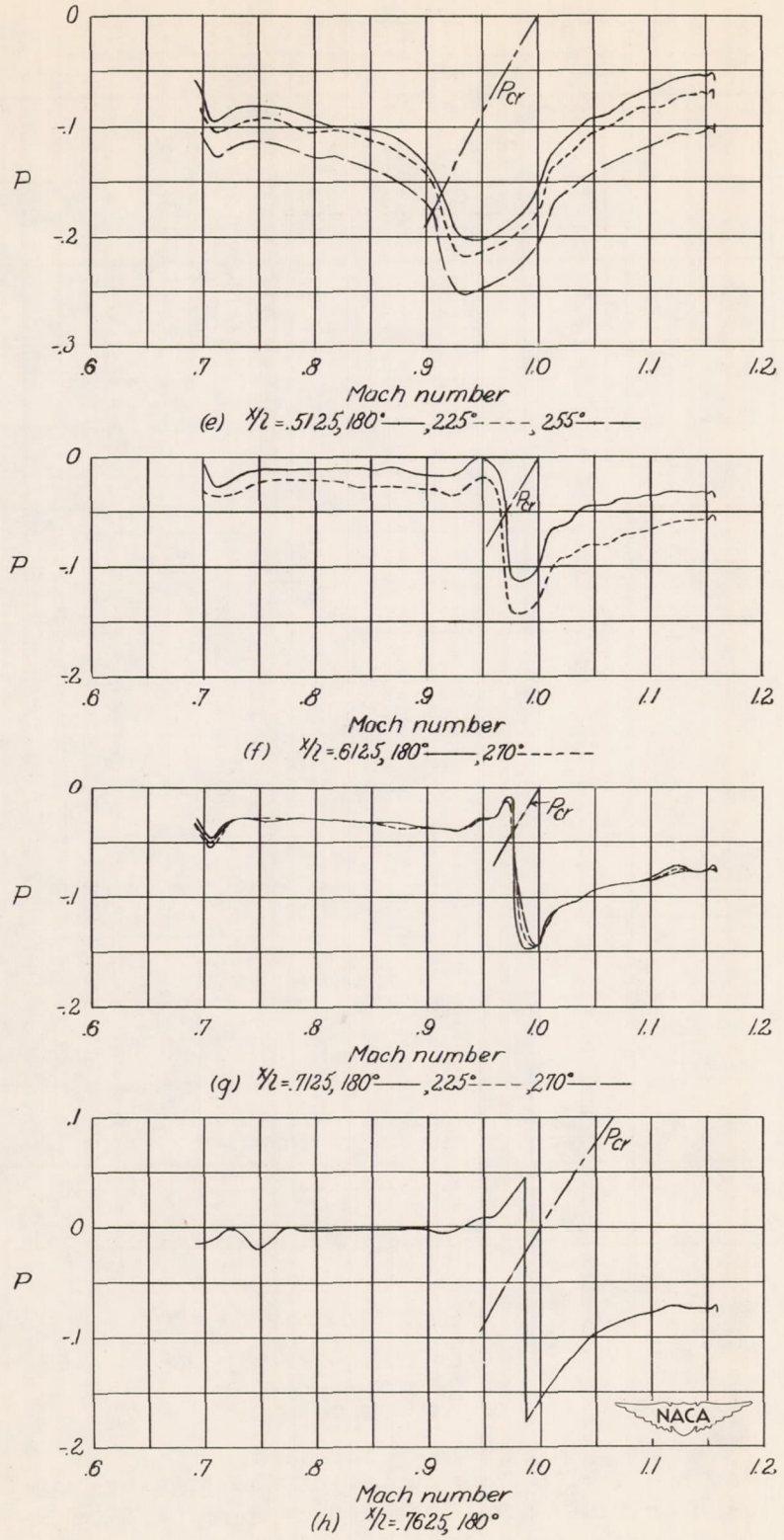

Figure 5.- Continued.

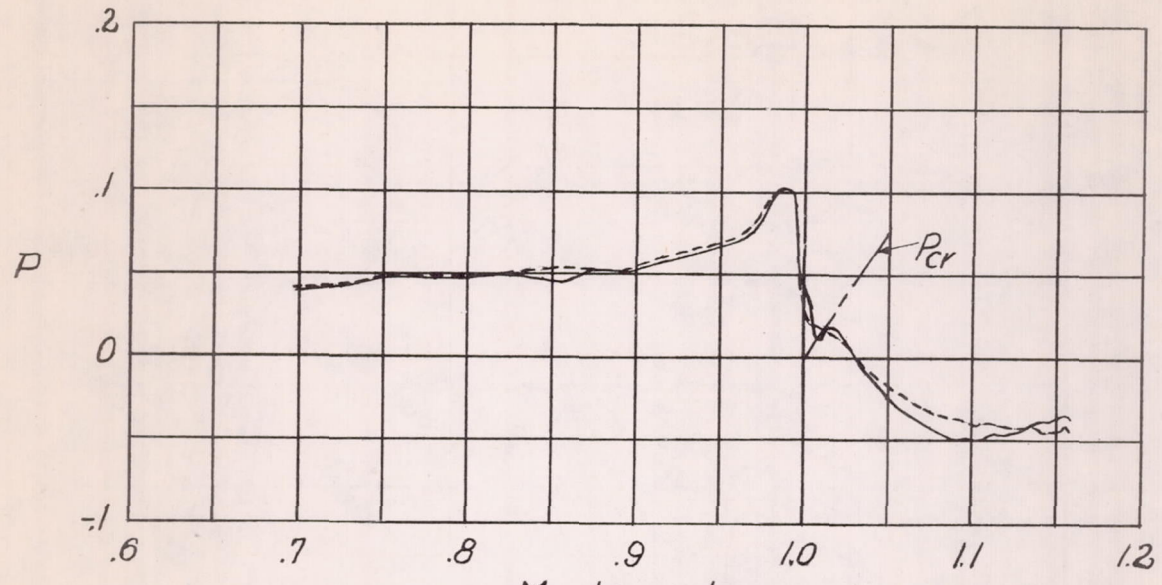

(i) x/l = .8125, 180° ——, 270° - - - -

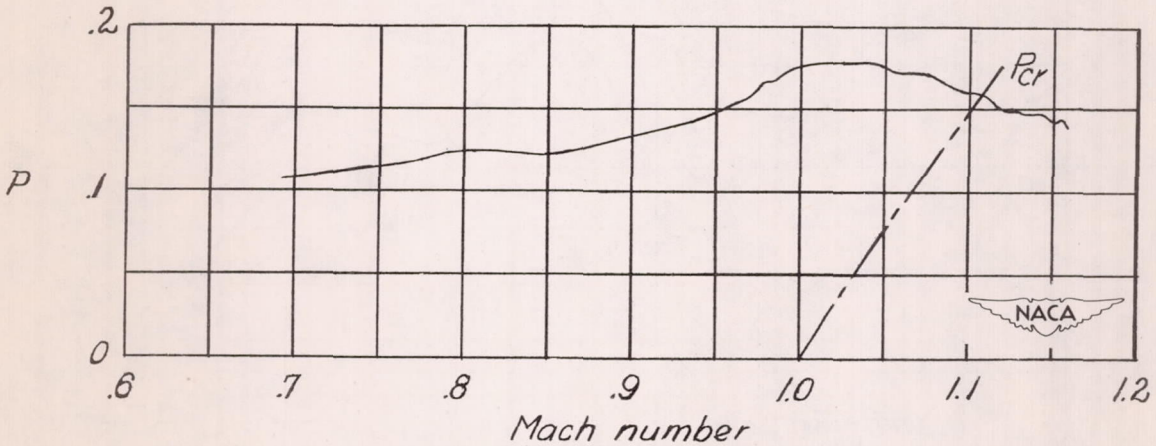

(j) x/l = .9021, 180°

Figure 5.- Concluded.

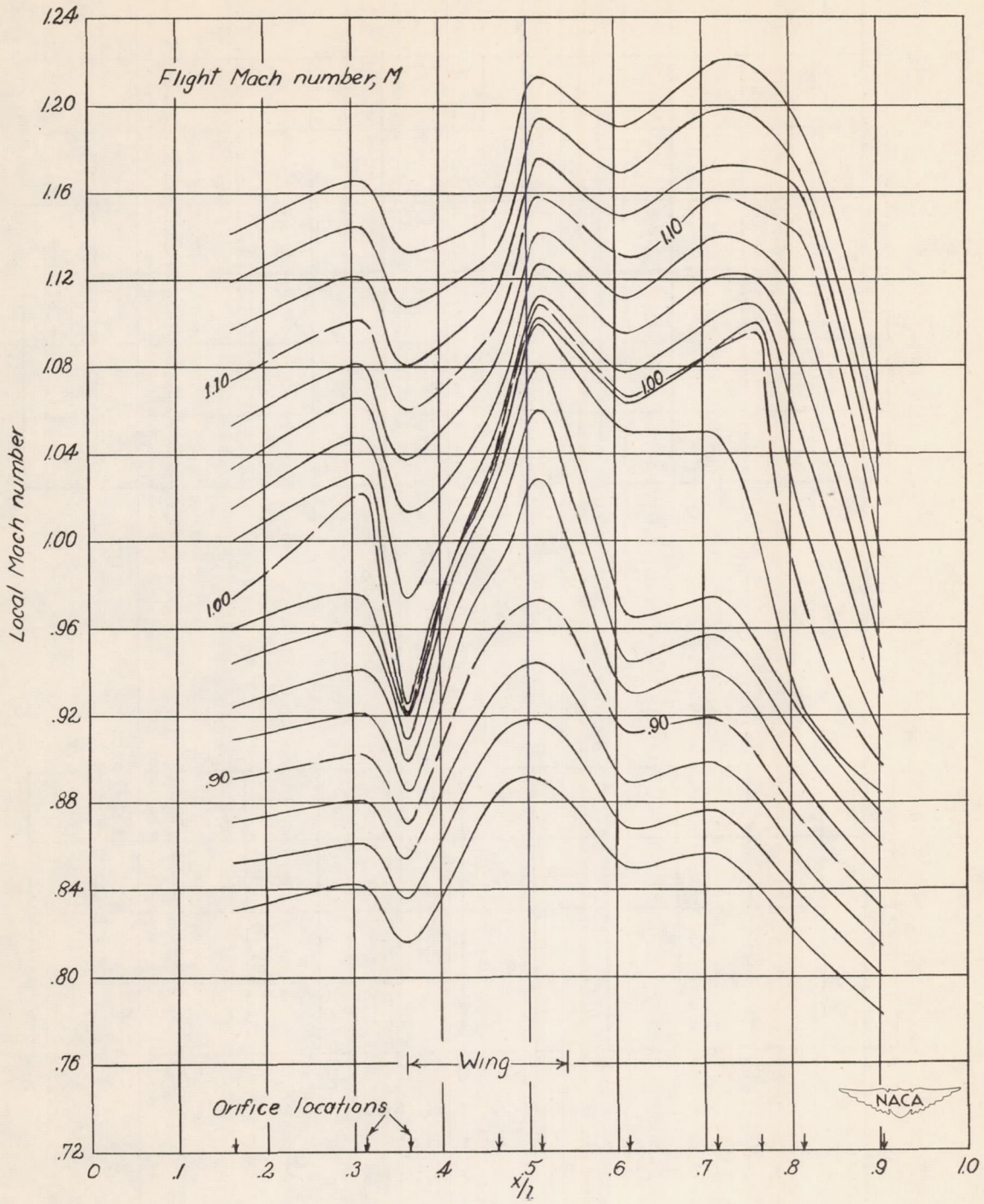

Figure 6.- The variation with position along the body x/l of the local Mach number for even values of free-stream Mach numbers. The wing and orifice locations are shown at the lower edge of the figure. The wing location shown is that of wing-body juncture.

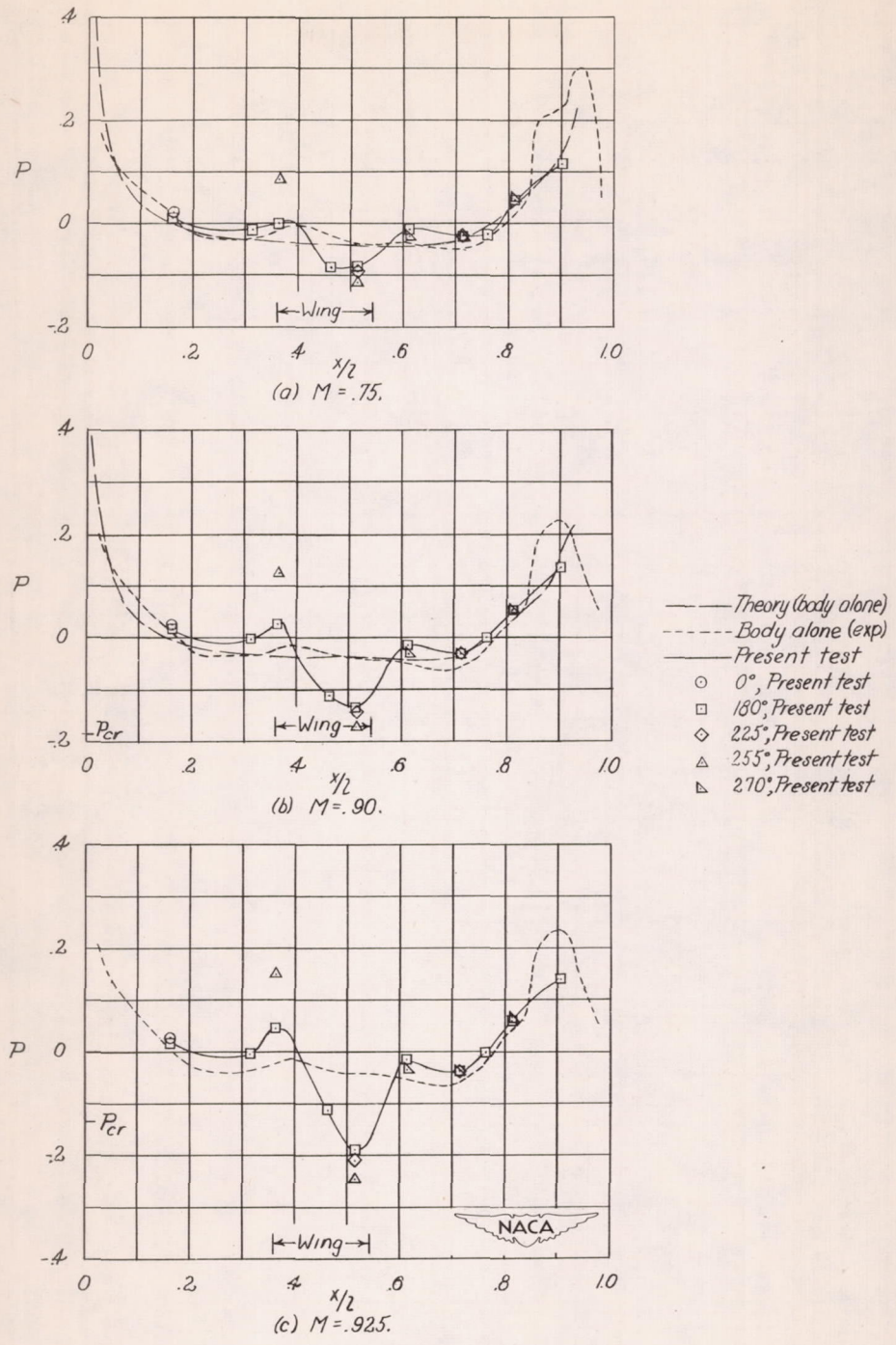

Figure 7.- Variation of pressure coefficient P with position along the body x/l for several Mach numbers. Included for comparison are measured (reference 1) and theoretical (references 1 and 8) distributions for the body alone. Also shown is P_{cr}, the pressure coefficient corresponding to local sonic velocity. The wing location shown is that of the wing-body juncture.

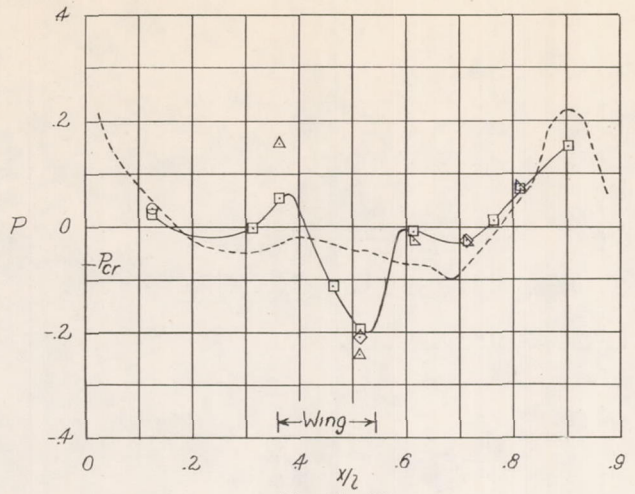

(d) M = .96.

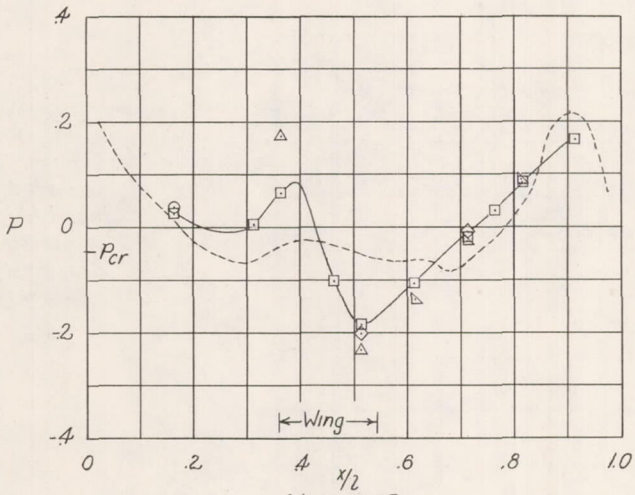

(e) M = .975.

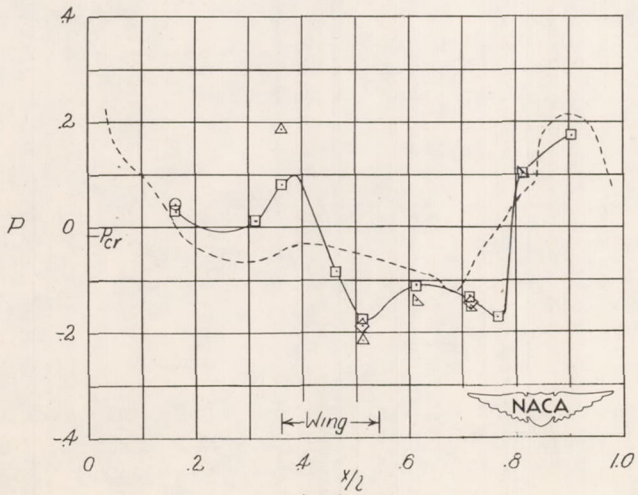

(f) M = .99.

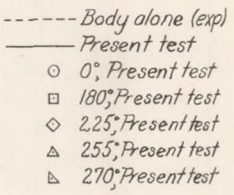

Figure 7.- Continued.

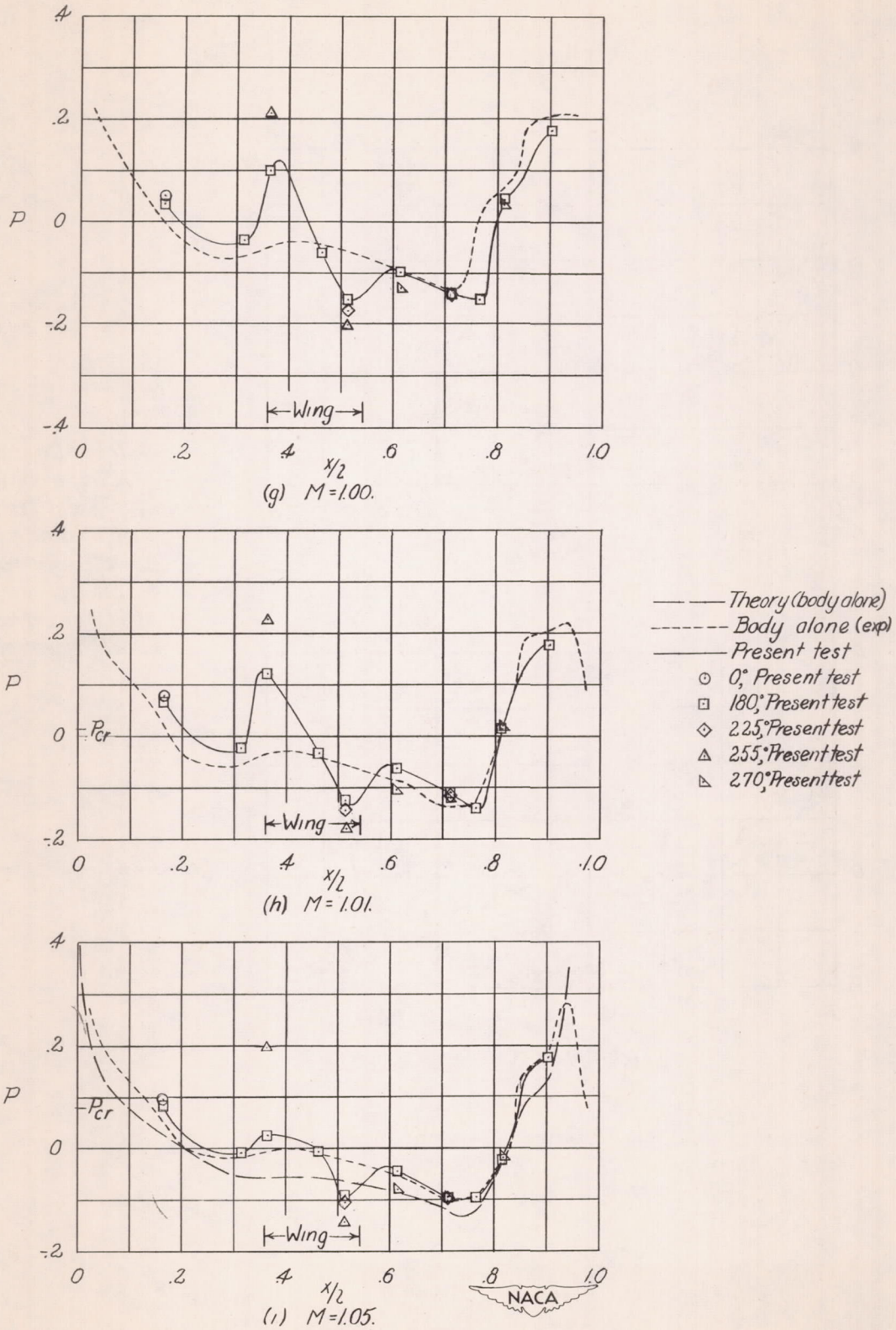

Figure 7.- Continued.

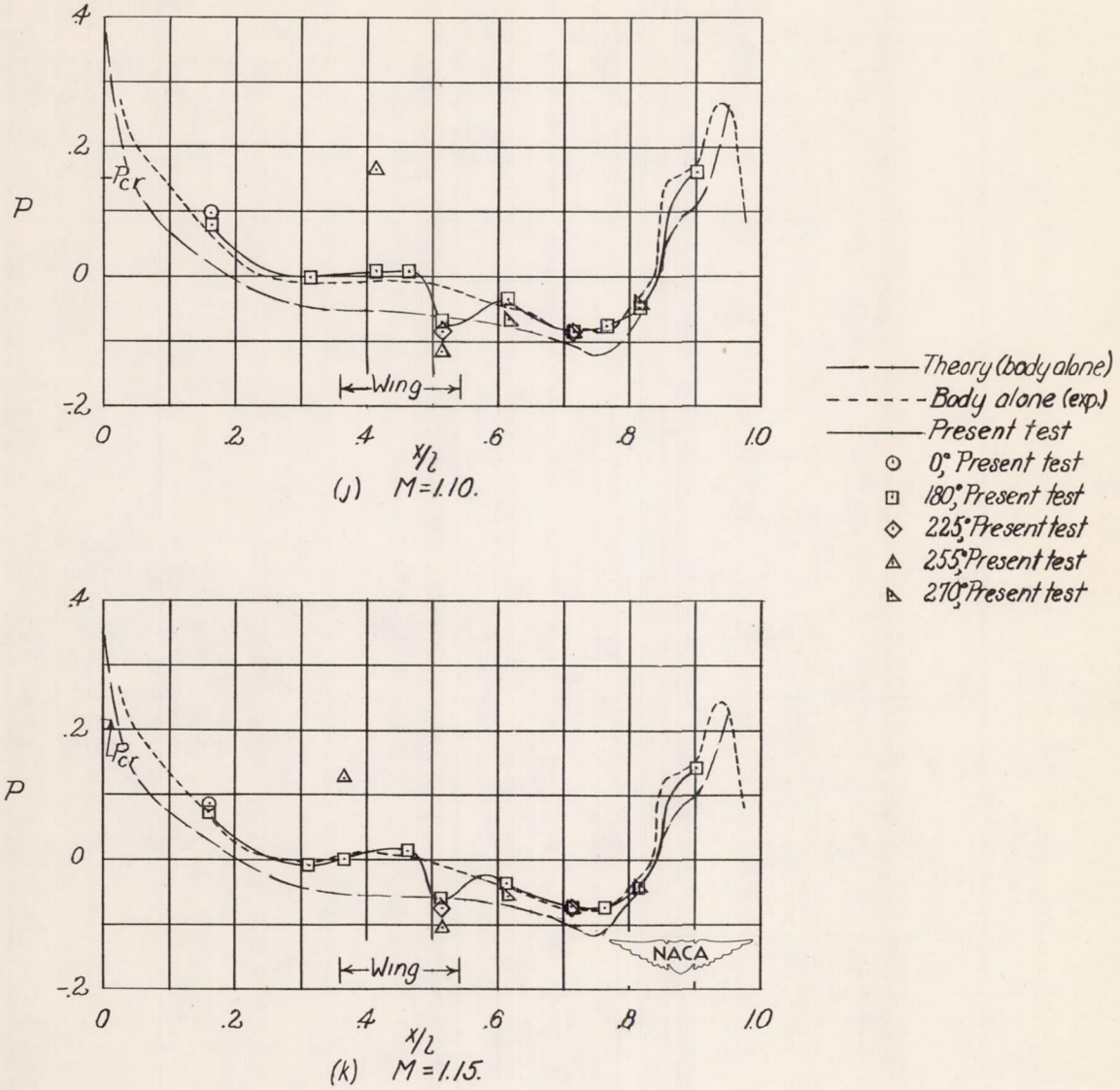

Figure 7.- Concluded.

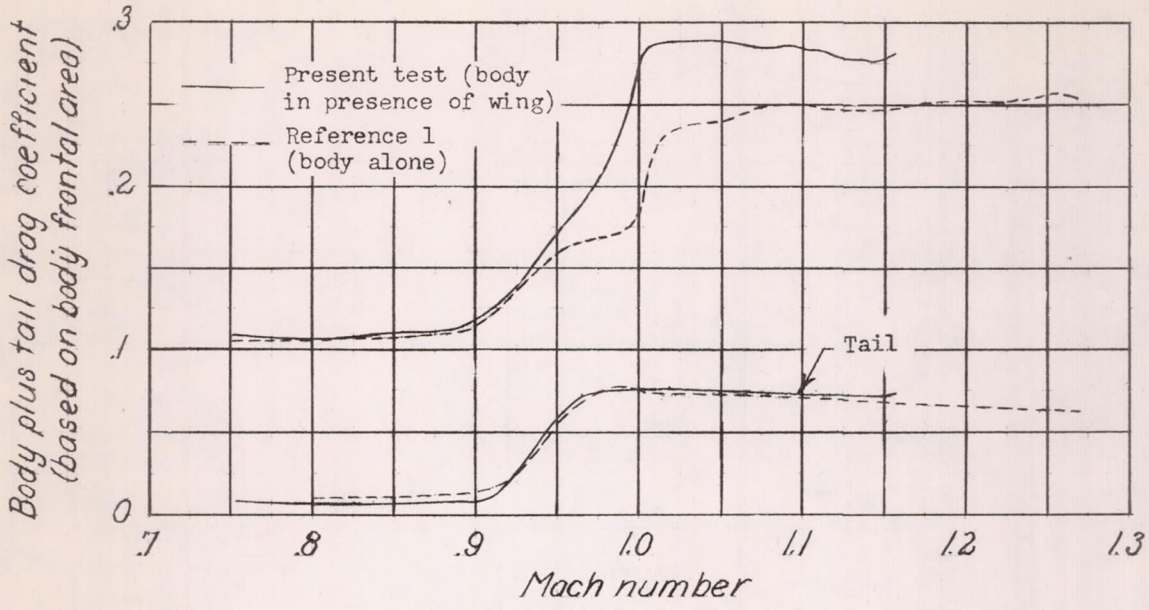

(a) Body-tail combination and tail.

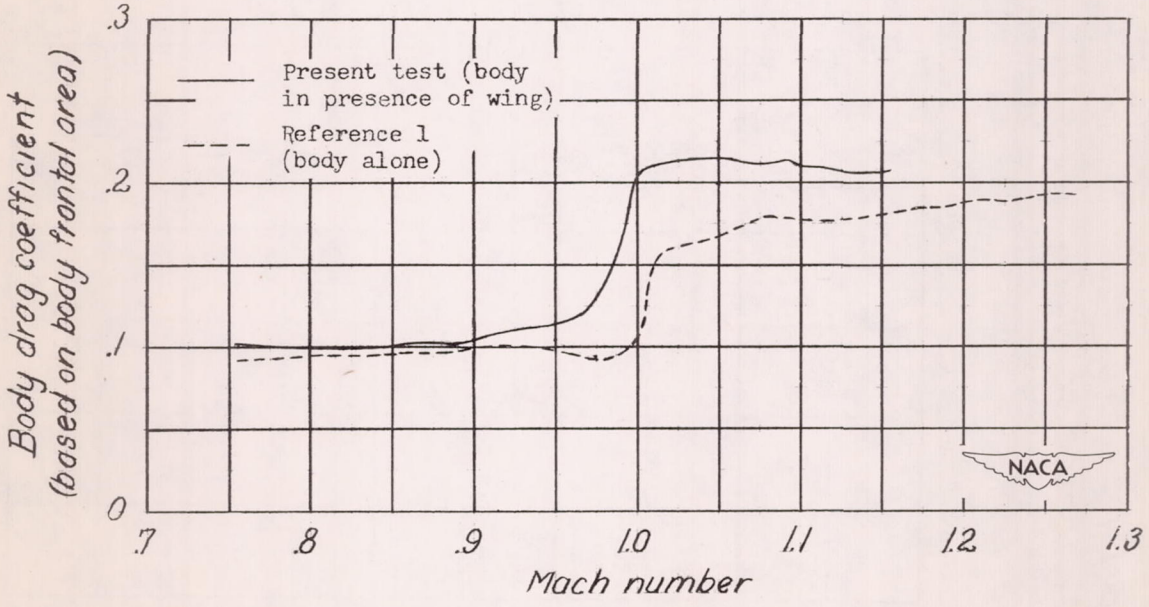

(b) Body.

Figure 8.- Variation with Mach number of drag coefficient for components of the wing-body combination and comparison with results for individual components.

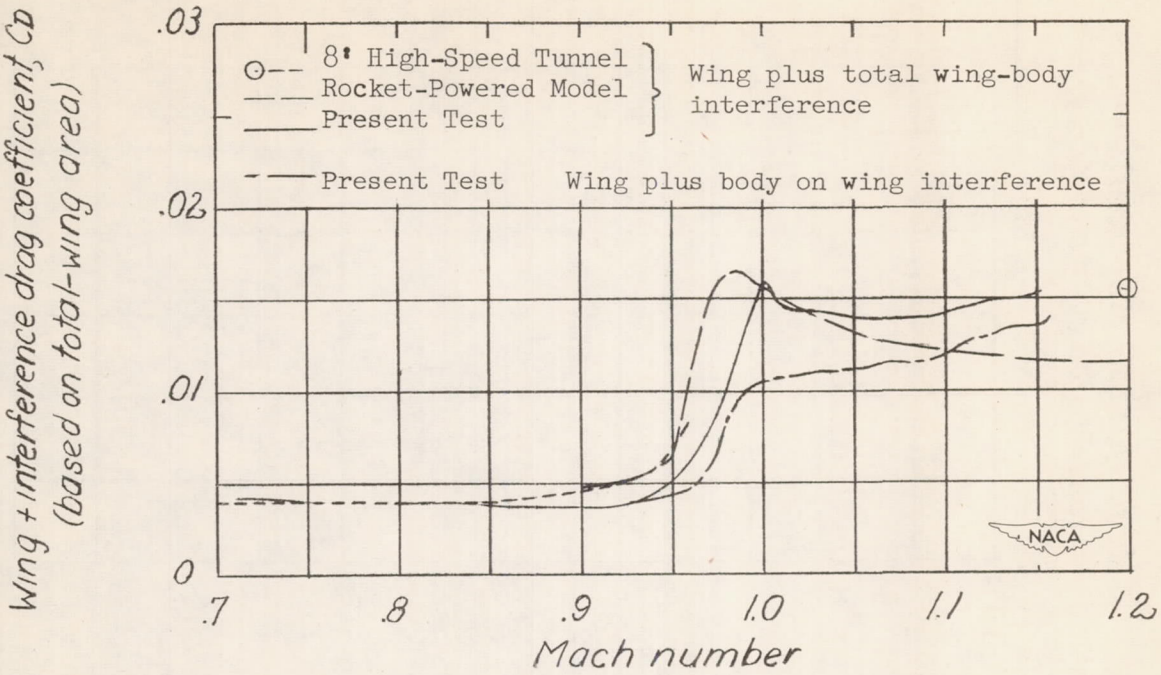

Figure 9.- Comparison of variations with Mach number of wing-plus-interference-drag coefficient obtained by different test techniques.

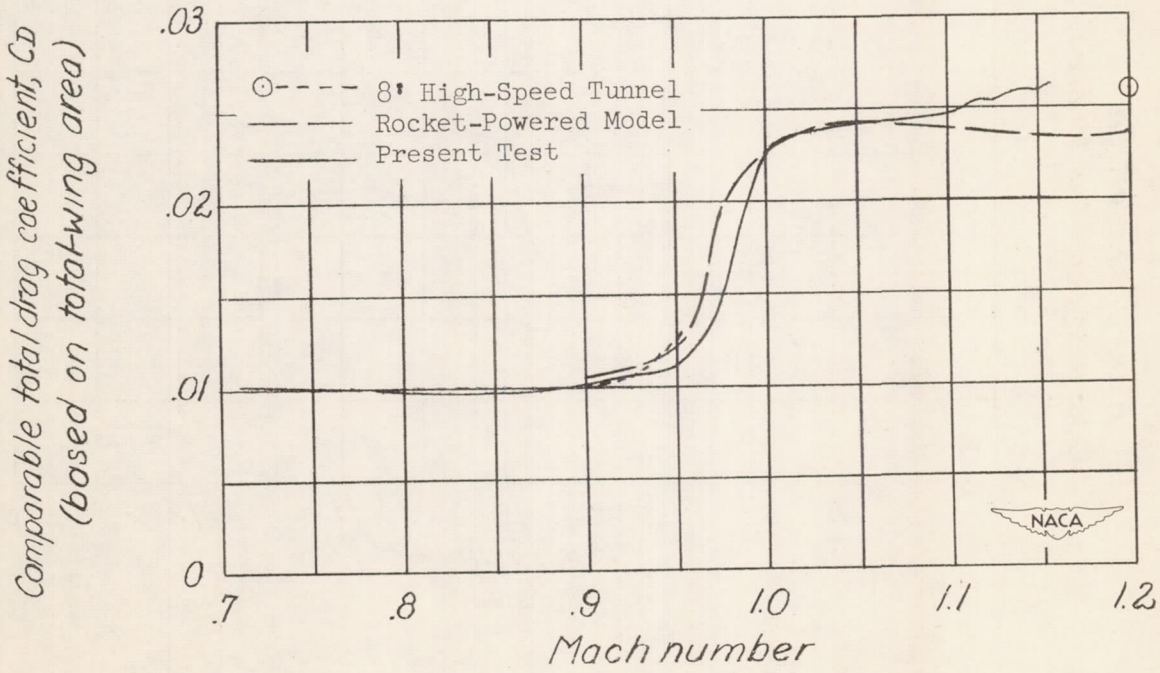

Figure 10.- Comparison of variations with Mach number of drag coefficients for the wing-body combination obtained by different test techniques.